

DST-GTN: Dynamic Spatio-Temporal Graph Transformer Network for Traffic Forecasting

Songtao Huang¹, Hongjin Song³, Tianqi Jiang⁴, Akbar Telikani⁵, Jun Shen⁵, Qingguo Zhou¹, Binbin Yong^{1,*} and Qiang Wu^{2,*}

¹Lanzhou University

²University of Electronic Science and Technology of China

³Northwestern University

⁴South China University of Technology

⁵University of Wollongong

{huangst21, zhouqg, yongbb}@lzu.edu.cn, hongjinsong2024@u.northwestern.edu, ctjiangtianqi@mail.scut.edu.cn, at952@uowmail.edu.au, jshen@uow.edu.au, qiang.wu@uestc.edu.cn

Abstract

Accurate traffic forecasting is essential for effective urban planning and congestion management. Deep learning (DL) approaches have gained colossal success in traffic forecasting but still face challenges in capturing the intricacies of traffic dynamics. In this paper, we identify and address these challenges by emphasizing that spatial features are inherently dynamic and change over time. A novel in-depth feature representation, called Dynamic Spatio-Temporal (Dyn-ST) features, is introduced, which encapsulates spatial characteristics across varying times. Moreover, a Dynamic Spatio-Temporal Graph Transformer Network (DST-GTN) is proposed by capturing Dyn-ST features and other dynamic adjacency relations between intersections. The DST-GTN can model dynamic ST relationships between nodes accurately and refine the representation of global and local ST characteristics by adopting adaptive weights in low-pass and all-pass filters, enabling the extraction of Dyn-ST features from traffic time-series data. Through numerical experiments on public datasets, the DST-GTN achieves state-of-the-art performance for a range of traffic forecasting tasks and demonstrates enhanced stability.

and the unpredictability of factors like road incidents or sudden weather shifts. Data-driven methods, such as the autoregressive integrated moving average (ARIMA) [Williams and Hoel, 2003] and the vector autoregressive model (VAR) [Lu *et al.*, 2016], generally treat traffic forecasting as a straightforward time series issue. These methods struggle with the high nonlinearity of traffic data because they rely on stationary assumptions, which are rarely met in actual traffic conditions.

The advent of deep learning (DL) [LeCun *et al.*, 2015] enabled the intricate capture of spatial-temporal correlations in traffic flows [Lv *et al.*, 2014; Li *et al.*, 2018]. Earlier DL-based approaches transformed traffic data into spatial-temporal (ST) grids, employing Convolutional Neural Networks (CNNs) to capture spatial dependencies and Recurrent Neural Networks (RNNs) for temporal dependencies [Yao *et al.*, 2018]. Recent DL studies focused on Spatio-Temporal Neural Graph Networks (STGNNs), which effectively utilize Graph Neural Networks (GNNs) to model the underlying graph structure of traffic data [Yu *et al.*, 2018; Wu *et al.*, 2019; Bai *et al.*, 2020]. Additionally, Spatio-Temporal Neural Networks (STNNs) based on self-attention mechanisms have emerged learning spatial and temporal relationships in a data-driven manner without prior knowledge [Zheng *et al.*, 2020; Park *et al.*, 2020; Jiang *et al.*, 2023].

As typical time series data, traffic data exhibit significant temporal dependency, as well as unique time-varying spatial relationships, which we refer to as ST dynamics. As shown in Figure 1, temporal dependency is a prominent characteristic in the traffic flow, with closer time points exhibiting stronger dependencies. On the other hand, spatial dependencies are continuously changing over time. Therefore, modeling both temporal dependencies and ST dynamics is crucial for accurate traffic forecasting. Previous DL-based approaches tend to model temporal and spatial information separately in an attempt to capture temporal and spatial dependencies [Wu *et al.*, 2019]. Moreover, in real-life scenarios, different functional areas at different times tend to have varying proportions of self-loop and adjacency relationship in graph structure, i.e., varying local and global information demands. Previous DL methods often overlook the varying needs of nodes for global

1 Introduction

With the rapid development of urbanization and the increasing number of vehicles, accurate traffic forecasting can aid in managing numerous traffic-related issues, such as congestion, travel duration, and flow control [Jin *et al.*, 2023a]. Traditional traffic forecasting studies are mainly categorized into knowledge-driven and data-driven methods [Shao *et al.*, 2022b]. Knowledge-driven methods, including queuing and traffic flow theories, simulate drivers' behavior [Cascetta, 2013]. However, they often overlook real-world complexities

*Corresponding author

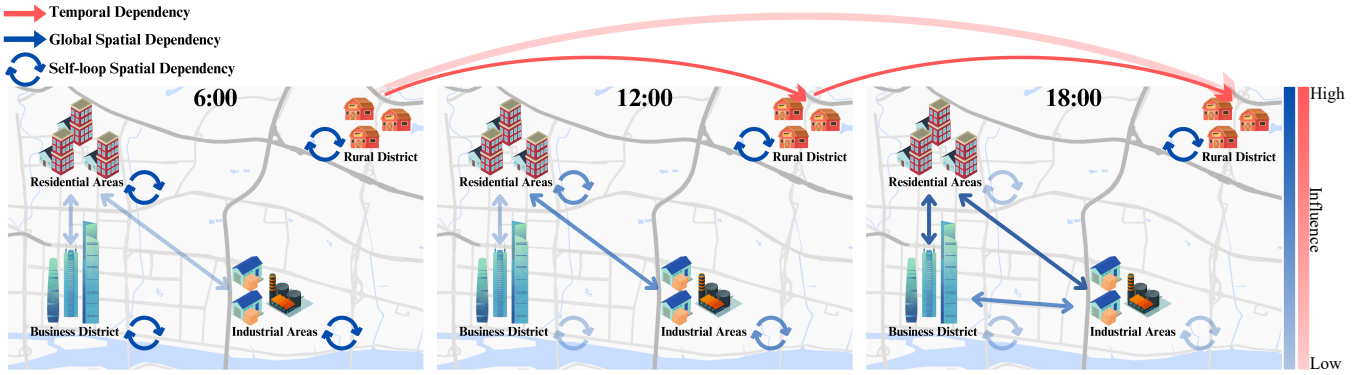


Figure 1: An example of a traffic flow system at three different times.

and local information in different ST scenarios, failing to capture the underlying dynamic ST characteristics of the traffic time-series data effectively.

To overcome these limitations, we introduce a Dyn-ST embedding to simulate time-varying spatial relationship in real-life traffic data and propose a Dynamic Spatio-Temporal Graph Transformer Network (DST-GTN) to dig out complex ST dynamics, based on the idea that ST dynamics are essentially superimposed on the temporal dimension. The main contributions of this work can be summarized as follows:

- We introduce a novel in-depth feature representation named Dynamic ST (Dyn-ST) features to simulate hidden ST dynamics in traffic time-series data and encapsulating time-varying spatial relationships.
- We propose a new traffic forecasting model named Dynamic Spatio-Temporal Graph Transformer Network (DST-GTN) to perform traffic forecasting accurately. Based on the idea that ST dynamics are superimposed on temporal dependencies, the DST-GTN can fully capture the complex ST dynamics in traffic time-series data. As the result, our method have a better performance.
- Extensive results show that our DST-GTN method achieves state-of-the-art (SOTA) performance and demonstrates competitive computational efficiency and robustness.

The remainder of this study is organized as follows: Section 2 presents related work on traffic forecasting. Fundamental concepts are investigated in Section 3. Section 4 introduces the details of proposed DST-GTN method. Section 5 conducts experiments across diverse real-world datasets. Section 6 concludes the paper.

2 Related Work

In this section, we summarize literature review related to traffic forecasting and introduce classic works of GNNs and Transformers and their applications in traffic forecasting.

2.1 Traffic Forecasting

Traditional work on traffic forecasting mostly falls into two categories: knowledge-driven and data-driven. Knowledge-driven approaches typically utilize queuing theory to simulate

user behavior in traffic, but often fail to account for the complex nature of real-world traffic flow [Cascetta, 2013]. Data-driven methods are usually based on statistical methods. For instance, ARIMA [Williams and Hoel, 2003] and VAR [Lu *et al.*, 2016] are used to forecast the traffic condition of each traffic sensor separately. However, these methods cannot handle the high non-linearity of each time series effectively. Furthermore, machine learning (ML) methods are proposed, such as support vector machine (SVM) [Drucker *et al.*, 1996] and k-nearest neighbor (KNN) [Van Lint and Van Hinsbergen, 2012], which are effective in relaxing the linear dependency assumption. Although these models mainly consider temporal dependencies and tend to overlook spatial relationships between traffic sensors. To model both temporal and spatial dependencies, deep learning (DL) methods, including Recurrent Neural Networks (RNNs) and Convolutional Neural Networks (CNNs), have been increasingly popular among researchers. In particular, these DL methods can extract latent representations and exploit much more features of traffic data than traditional ML methods [Bui *et al.*, 2022]. Nonetheless, they are not optimal for traffic forecasting because road networks possess graph structure. Therefore, recent works in this field of study feature graph-based DL methods that capture the graph structure in traffic time-series data, such as STGNNs [Wu *et al.*, 2019] and STNNs [Zheng *et al.*, 2020].

2.2 Graph Neural Network

Graph Neural Networks (GNNs) are useful tools for learning spatial dependencies. Common GNNs can be divided into three categories: spectral-based GCNs, spatial-based GCNs and GATs [Jin *et al.*, 2023b]. Spectral-based GCNs, as exemplified in [Bruna *et al.*, 2014], introduce filters from graph signal processing in the spectral domain to define the graph convolution process. Among the spectral-based GCNs, ChebNet [Defferrard *et al.*, 2016] leverages a truncated expansion of Chebyshev polynomials up to the k^{th} order to reduce the complexity of Laplacian computation. Furthermore, GCN [Kipf and Welling, 2017], a first-order approximation of ChebNet, achieves outstanding performance in a variety of tasks. On the other hand, spatial-based GCNs, define the graph convolution process through information propagation. Diffusion graph convolution (DGC) [Atwood and Towsley, 2016] employs a transition probability from one node to its

neighboring nodes to simulate graph convolution process. GraphSAGE [Hamilton *et al.*, 2017] uses sampling to obtain a fixed number of neighbors and models the graph convolutions as an information-passing process from one node to another directly connected node. To dynamically learn the importance of neighbor nodes in learning spatial dependencies, GAT [Veličković *et al.*, 2018] integrates the attention mechanism into the node aggregation operation. Recently, GCNs has been adopted as a common component in STGNNs to model spatial relationships in ST data. DCRNN [Li *et al.*, 2018] and STGCN [Yu *et al.*, 2018] employed predefined graphs to capture spatial dependencies and adopt RNNs or CNNs to model temporal features. Additionally, some studies, such as STSGCN [Song *et al.*, 2020] and STFGNN [Li and Zhu, 2021], have attempted to simultaneously model temporal and spatial relationships by designing ST graphs.

2.3 Transformer

Transformer [Vaswani *et al.*, 2017], a self-attention based architecture, was initially applied to natural language processing (NLP) tasks and has achieved extraordinary performance across multiple NLP tasks [Devlin *et al.*, 2019]. In addition to its success in natural language processing, the Transformer architecture has demonstrated promising results in computer vision tasks, as evidenced by models like Vision Transformer [Ruan *et al.*, 2022] and Swin Transformer [Liu *et al.*, 2021]. In traffic forecasting, Transformer architecture based STNNs has also demonstrated outstanding competitive capabilities. GMAN [Zheng *et al.*, 2020] employed an encoder-decoder architecture consisting of multiple ST attention blocks to model the impact of ST dynamics. PDFormer [Jiang *et al.*, 2023] adopts multiple self-attention mechanisms with different design perspectives in its encoder to capture both temporal and spatial dependencies. Similarly, STAEformer [Liu *et al.*, 2023] utilized the encoder of the Vanilla Transformer, applying it from both temporal and spatial perspectives.

3 Preliminaries

In this section, we first introduce background knowledge of our work, including GCN and Transformer. Next, we define the traffic network, traffic time-series data and multi-step traffic forecasting problem addressed.

3.1 Preliminary of GCN

Spectral-based GCNs [Bruna *et al.*, 2014] are a class of classical models of GCNs. Spectral-based GCNs, i.e. GCN [Kipf and Welling, 2017] offering a more efficient approach to graph convolution, formulate the propagation rule with

$$Z^{(l+1)} = \left(I + D^{-\frac{1}{2}} A D^{\frac{1}{2}} \right) Z^{(l)} \theta, \quad (1)$$

where I is the identity matrix and A is the adjacency matrix, with θ representing the learnable parameters. In a GCN, $D^{-\frac{1}{2}} A D^{\frac{1}{2}}$ can be considered a low-pass filter to obtain global information of given graph, while I serves as an all-pass filter to capture local information. AKGNN [Ju *et al.*, 2022]

transforms the GCN into

$$Z^{(l+1)} = \left(\frac{2\lambda_{\max}^l - 2}{\lambda_{\max}^l} I + \frac{2}{\lambda_{\max}^l} D^{-\frac{1}{2}} A D^{\frac{1}{2}} \right) Z^{(l)} \theta, \quad (2)$$

where $\lambda_{\max}^l \in (1, +\infty)$ is a learnable scalar used to control the low-pass and all-pass filters. When $\lim \lambda_{\max}^l \rightarrow 1$, the form is approximated by $Z^{(l+1)} = \left(2D^{-\frac{1}{2}} A D^{\frac{1}{2}} \right) Z^{(l)} \theta$, which represents a full low-pass filter and only considers global information. When $\lim \lambda_{\max}^l \rightarrow \infty$, the form is approximated by $Z^{(l+1)} = (2I) Z^{(l)} \theta$, which represents a full all-pass filter and only considers local information.

3.2 Preliminary of Transformer

The Transformer described in [Vaswani *et al.*, 2017] is composed of multiple Transformer blocks, each containing a self-attention component and a position-wise feed-forward network (FFN) component. After each component, residual connections and layer normalization are typically applied. Assuming that the input to the l^{th} Transformer block is $Z^{(l)} \in \mathbb{R}^{T^T \times D}$, the self-attention process on $Z^{(l)}$ can be computed by

$$Q = Z^{(l)} W^Q, \quad K = Z^{(l)} W^K, \quad V = Z^{(l)} W^V \quad (3)$$

$$\text{Attention}(Q, K, V) = \text{softmax} \left(\frac{QK^T}{\sqrt{d_K}} \right) V \quad (4)$$

where $W^Q, W^K \in \mathbb{R}^{T^D \times d_K}, W^V \in \mathbb{R}^{T^D \times d_V}$ are learnable parameters used to map $Z^{(l)}$ to queries, keys and values, respectively.

3.3 Problem Definition

Definition 1 (Traffic Network). *A traffic network can be represented as either a directed or undirected graph $G = (V, E, A)$, where V represents a set of traffic sensor nodes with a total of N nodes ($|V| = N$), E is a set of edges between these nodes, and $A \in \mathbb{R}^{N \times N}$ is an adjacency matrix indicating the reachability between sensor nodes.*

Definition 2 (Traffic Time-Series Data). *We denote $X_t \in \mathbb{R}^{N \times C}$ as traffic time-series data collected from N traffic sensor nodes at time t , where traffic time-series data can represent either traffic flow or traffic speed. In our study, C equals 1.*

Definition 3 (Multi-step Traffic Forecasting). *Given a historical traffic data sequence $\mathcal{X} = (X_{t-T}, X_{t-T+1}, \dots, X_t) \in \mathbb{R}^{T \times N \times C}$, our aim is to predict the future traffic data sequence $[X_{t+1}, X_{t+2}, \dots, X_{t+T}] \in \mathbb{R}^{T \times N \times C}$ based on the observed historical values, i.e. multi-step traffic forecasting. We formulate the problem as finding a mapping function f to forecast the next T steps traffic time-series data based on the previous T steps traffic time-series data, that is*

$$[X_{t+1}, X_{t+2}, \dots, X_{t+T}] = f(X_{t-T+1}, X_{t-T}, \dots, X_t). \quad (5)$$

4 Methods

In this section, we introduce our Dynamic Spatio-Temporal Graph Transformer Network (DST-GTN) model. We describe its architecture and the details of DST-GTN.

4.1 Architecture of DST-GTN

We introduce the architecture of proposed Dynamic Spatio-Temporal Graph Transformer Network (DST-GTN) in Figure 2. Specifically, The four main modules of the frame are summarized as follows:

- **Embedding Layer:** it generates traffic data embedding, temporal identity embedding and Dyn-ST embedding.
- **Temporal Transformer Module:** it captures different hidden temporal dependencies along the time dimension.
- **Dynamic Spatio-Temporal Module:** it comprises two components: the Dynamic Spatio-Temporal Graph Generator (DSTGG) and the Node Frequency Learning Spatio-temporal Graph Convolution Network (NFL-STGCN). The DSTGG captures time-varying spatial relationships represented in Dyn-ST embedding. The NFL-STGCN component learns the global and local information demands of nodes in different ST scenarios. These two components jointly address the limitation mentioned in Introduction.
- **Output Layer:** it forecasts all time slices for all nodes simultaneously utilizing the ST information generated by the past three parts.

4.2 Modules of DST-GTN

We detail about each module of DST-GTN.

Embedding Layer

We introduce two types of embedding in Embedding Layer: Temporal Identity Embedding and Dynamic Spatio-Temporal (Dyn-ST) Embedding, to jointly represent complex relationship of traffic data.

- **Temporal Identity Embedding.** In order to enhance temporal distinguishability, we design two additional temporal identity embeddings $E^{week} \in \mathbb{R}^{T \times d_1}$ and $E^{day} \in \mathbb{R}^{T \times d_1}$ to jointly identify the traffic characteristics at a certain moment. Specifically, E^{week} captures the temporal characteristics related to weekly periodicity, while E^{day} focuses on daily periodicity. The detailed generation process of them is described in Appendix A.1.
- **Dynamic Spatio-Temporal Embedding.** We introduce a dynamic spatio-temporal (Dyn-ST) embedding, denoted as $E^{st} \in \mathbb{R}^{N \times T \times d_2}$, to simulate the complex ST dynamics in traffic data. Here d_2 is the embedding dimension of E^{st} . Note that E^{st} is a randomly initialized trainable tensor, which is progressively updated during the training process to accurately represent the ST dynamics.

Raw traffic time-series data \mathcal{X} are transformed into a high-dimensional representation $\mathcal{H} \in \mathbb{R}^{T \times N \times d}$ through a fully connected layer, where d is the embedding dimension. The output of embedding layer is generated by concatenating the traffic data embedding, the temporal identity embedding, and the Dyn-ST embedding, as shown in the equation:

$$\mathcal{Z} = \mathcal{H} \| E^{day} \| E^{week} \| E^{st}, \quad (6)$$

where $\mathcal{Z} \in \mathbb{R}^{N \times T \times D}$ and $D = d + 2d_1 + d_2$. This output is then used as the input for the following Temporal Transformer module.

Temporal Transformer Module

To capture global temporal dependencies of embedded traffic data, we adopt Transformer blocks in Vanilla Transformer [Vaswani *et al.*, 2017] to form Temporal Transformer module. Each Temporal Transformer module contains two components: multi-head temporal self-attention (MTSA) and a position-wise feed-forward network (FFN). Define the representation of the embedding data \mathcal{Z} at the i^{th} traffic sensor as $Z^i \in \mathbb{R}^{T \times D}$, $i \in \{1, \dots, N\}$. In MTSA component, Z^i is firstly converted to query matrices $Q^i \in \mathbb{R}^{T \times d_K}$, key matrices $K^i \in \mathbb{R}^{T \times d_K}$, and value matrices $V^i \in \mathbb{R}^{T \times d_V}$ by matrix multiplication. The temporal self-attention (TSA) process on node i can be calculated as:

$$Q^i = Z^i W^{Q^i}, K^i = Z^i W^{K^i}, V^i = Z^i W^{V^i} \quad (7)$$

$$TSA_i(Q^i, K^i, V^i) = softmax\left(\frac{Q^i K^{i\top}}{\sqrt{d_K}}\right) V^i \quad (8)$$

where $W^Q \in \mathbb{R}^{D \times d_K}$, $W^K \in \mathbb{R}^{D \times d_K}$, $W^V \in \mathbb{R}^{D \times d_V}$ are learnable parameter. For simplicity, we set $d_K = d_V = D$. Due to the different temporal dependencies of traffic data sequences, we expand TSA to multi-head version with h head, i.e., MTSA. Query, key, and value are split into h heads in the embedding dimension, which can be denoted as $Q_m^i, K_m^i, V_m^i \in \mathbb{R}^{T \times \frac{D}{h}}$, $m \in \{1, \dots, h\}$. The calculation process of MTSA on node i is denoted as:

$$MTSA_i(Q^i, K^i, V^i) = W^O * Concat(head_1, \dots, head_h) \quad (9)$$

$$where head_m = TSA(Q_m^i, K_m^i, V_m^i)$$

We employ MTSA in parallel for all nodes on \mathcal{Z} and concatenate all outputs in the node dimension. Therefore, the MTSA process on \mathcal{Z} can be represented as:

$$MTSA(\mathcal{Z}) = Concat(MTSA_1(Q^1, K^1, V^1), \dots, MTSA_N(Q^N, K^N, V^N)) \quad (10)$$

The FFN is implemented by multiple fully connected layers and closely follows MTSA's usage. Following vanilla Transformer, we adopt layer normalization (LayerNorm) after each MTSA component and FFN component. The overall process of l^{th} Temporal Transformer module can be calculated as:

$$\hat{\mathcal{Z}}^{(l)} = LayerNorm(MTSA(\mathcal{Z}^{(l-1)}) + \mathcal{Z}^{(l-1)}) \quad (11)$$

$$\mathcal{Z}^{(l)} = LayerNorm(FFN(\hat{\mathcal{Z}}^{(l)}) + \hat{\mathcal{Z}}^{(l)}) \quad (12)$$

The output of the last Temporal Transformer block is denoted as \mathcal{Z} as before for simplicity, which will be fed into DSTM.

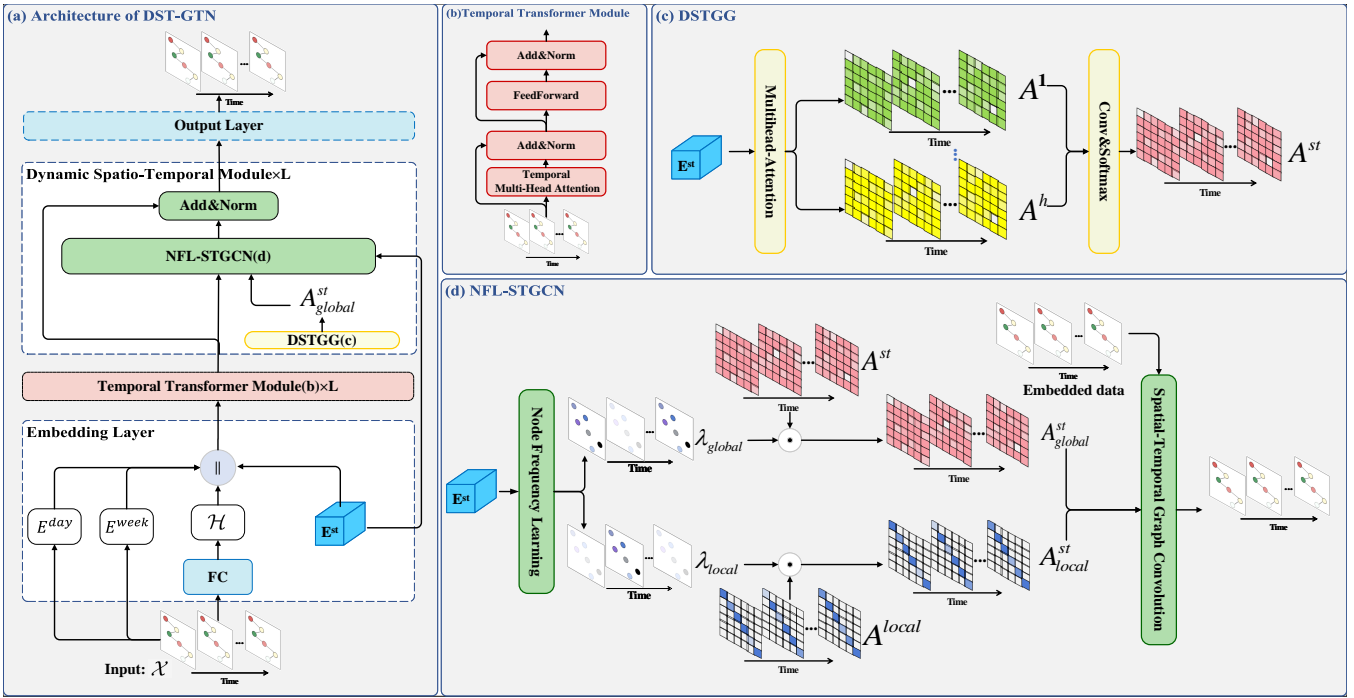


Figure 2: The detailed architecture of DST-GTN. (a) represents the overall architecture of DST-GTN. (b) describes the Temporal Transformer Module, which captures temporal dependencies in the embedded data. (c) illustrates the Dynamic Spatio-Temporal Graph Generator (DSTGG) component of the Dynamic Spatio-Temporal Module (DSTM), which utilize Dyn-ST embedding to generate a global ST graph. (d) is the NFL-STGCN component of the DSTM, which adaptively learns the local and global information demand for each ST node to adjust the ST graph. The optimized two ST graph is finally employed in the ST graph convolution process.

Dynamic Spatio-Temporal Module

In the Dynamic Spatio-Temporal Module (DSTM), a DSTGG component utilize Dyn-ST embedding to construct a global ST graph. Following this, a NFL-STGCN component learn the demand of each ST nodes for local and global information. This learned information is used to refine the global and local ST graphs accordingly. The optimized two ST graph is finally employed in the ST graph convolution process.

- **DSTGG.** Considering Dyn-ST embedding $E^{st} \in \mathbb{R}^{T \times N \times d_2}$ can simulate the ST dynamics of real-world traffic time-series data, we can employ E^{st} to capture the time-varying spatial relationships of traffic data, which can be represented by a ST graph. First, denoting the representation of E^{st} at time t is $E_t^{st} \in \mathbb{R}^{N \times d_2}$, the global spatial relationship of sensor nodes at time t can be calculated using spatial self-attention (SSA) on E_t^{st}

$$Q_t = E_t^{st} W^{Q_t}, K_t = E_t^{st} W^{K_t} \quad (13)$$

$$SSA_t(Q_t, K_t) = \frac{Q_t K_t^\top}{\sqrt{d_2}} \quad (14)$$

where $Q_t, K_t \in \mathbb{R}^{N \times d_k}$ are query and key matrix of at time t and $W^{Q_t}, W^{K_t} \in \mathbb{R}^{d_2 \times d_k}$, $d_k = d_2$ are learnable parameters. Note that different with the TSA component in Temporal Transformer module, here we only calculate the unnormalized attention matrix to express the spatial relationship. However, one spatial relationship

is not enough. Spatial relationships in traffic data often exhibit multiple patterns, such as distance relationships and functional area relationships. To explicitly model different spatial patterns, we expand the aforementioned SSA into h heads, with each head representing a possible spatial relationship:

$$A_t^1, \dots, A_t^h = SSA_1(Q_t^1, K_t^1), \dots, SSA_h(Q_t^h, K_t^h) \quad (15)$$

where $Q_t^m, K_t^m \in \mathbb{R}^{N \times \frac{d_2}{h}}$, $m \in \{1, \dots, h\}$ is the query, key of m^{th} head, and $A_t^m \in \mathbb{R}^{N \times N}$ represent attention matrix of m^{th} spatial pattern at time t . In this way, we can compute h different attention matrix $\{A_t^1, \dots, A_t^h\}$ to represent h different spatial pattern at time t . Then, we integrate the information of h spatial attention matrix through convolution operation and normalize it to generate a normalized adjacency matrix at time t :

$$A_t = softmax(Conv(A_t^1, \dots, A_t^h)) \quad (16)$$

where the convolution operation uses $h * 1$ convolution kernels to simultaneously mix the information of h attention matrices.

We perform the aforementioned calculations in parallel at all time points to generate T global spatial graph, and finally concatenate them along the time dimension to form a global ST graph $A^{st} \in \mathbb{R}^{T \times N \times N}$ that represents global ST relationships.

$$A^{st} = (A_1 ||, \dots, || A_T) \quad (17)$$

The entire process of generating a global ST graph A^{st} is defined as Dynamic Spatio-Temporal Graph Generator (DSTGG).

- **NFL-STGCN.** In traffic data, different traffic sensor nodes often have different demands for global and local information. For instance, suburban nodes, which interact less with the outside, are more focused on local information, while those in urban centers, having frequent interactions with neighboring nodes, require a greater emphasis on global information. In addition, this characteristic tends to change over time.

To model these characteristics, inspired by AKGNN [Ju *et al.*, 2022], we can assign different all-pass filter weights and low-pass filter weights for each node during graph convolution process, tailored to their specific ST contexts.

Specifically, we first utilize Dyn-ST embedding E^{st} to learn expected all-pass filter weights and low-pass filter weights for each node, namely Node Frequency Learning (NFL):

$$\lambda = 1 + ReLU(MLP(E^{st})) \quad (18)$$

$$\lambda_{local} = \frac{2\lambda - 2}{\lambda}, \lambda_{global} = \frac{2}{\lambda} \quad (19)$$

where $\lambda, \lambda_{local}, \lambda_{global} \in \mathbb{R}^{T \times N}$, and MLP is 2-layer fully connected layer with $ReLU$ activation. $\lambda_{local}, \lambda_{global}$ indicate the expected all-pass and low-pass filter weights of each sensor nodes, respectively, which is uncovered in a data driving way. Note that the sum of λ_{local} and λ_{global} is 2. When λ is greater than 1, the model expect all-pass filter can dominate. When λ is less than 1, it expect low-pass filter takes precedence.

After learn expected all-pass filter weights and low-pass filter weights for each node, we denote a local ST graph $A^{local} \in \mathbb{R}^{T \times N \times N}$ as a all-pass filter, which is generated by concatenating T identity matrix with shape $N \times N$. The global ST graph A^{st} generated by previous DSTGG can be considered as a low-pass filter. We can use expected all-pass filter weights and expected low-pass filter weights to adjust these two filter:

$$A_{local}^{st} = \lambda_{local} \odot A^{local}, A_{global}^{st} = \lambda_{global} \odot A^{st} \quad (20)$$

where \odot represent element-wise multiplication and the missing dimensions of $\lambda_{local}, \lambda_{global}$ will be broadcasted when element-wise multiplication

Then, defining the representations of $A_{local}^{st}, A_{global}^{st}$ generated at the l^{th} layer as $A_{local}^{st(l)}, A_{global}^{st(l)}$, we can expand spectral graph convolution to ST graph convolution to aggregate ST information of traffic data:

$$\hat{\mathcal{Z}}^{(l)} = (A_{local}^{st(l)} + A_{global}^{st(l)}) \times \mathcal{Z}^{(l-1)} W \quad (21)$$

where \times represents tensor multiplication and $W \in \mathbb{R}^{D \times D}$ is a learnable parameter. $\mathcal{Z}^{(l-1)} \in \mathbb{R}^{T \times N \times D}$ is the output of $l - 1^{th}$ layer and $\hat{\mathcal{Z}}^{(l)} \in \mathbb{R}^{T \times N \times D}$ is the ST convolution result in l^{th} layer. The tensor multiplication can be viewed as performing graph convolution in parallel on different time slices.

We stack L DSTM. In l^{th} DSTM, assuming the output of NFL-STGCN is $\hat{\mathcal{Z}}^{(l)}$, we employ residual connection and layer normalization to generate the final output $\mathcal{Z}^{(l)}$ of l^{th} DSTM:

$$\mathcal{Z}^{(l)} = LayerNorm(\hat{\mathcal{Z}}^{(l)} + \mathcal{Z}^{(l-1)}) \quad (22)$$

Output Layer

Finally, we directly employ a MLP to transform the output of last DSTM to the expected forecasting sequence $\mathcal{Y} \in \mathbb{R}^{T \times N \times C}$, which can be represented as:

$$\mathcal{Y} = MLP(\mathcal{Z}^{(L)}) \quad (23)$$

where $\mathcal{Z}^{(L)} \in \mathbb{R}^{T \times N \times D}$ is the output of the last DSTM.

5 Experiments

In this section, we compared the proposed DST-GTN with state-of-the-art models on five real-world traffic datasets. We design comprehensive ablation studies to evaluate the impact of each module. Finally, we analyze the computational efficiency and robustness of DST-GTN.

5.1 Datasets

We assessed the performance of DST-GTN using five publicly available real-word public traffic datasets: PEMS04, PEMS07, PEMS08, PEMS07(M) and PEMS07(L), which were collected from the Caltrans Performance Measurement System (PeMS) [Chen *et al.*, 2001]. Among them, PEMS04, PEMS07, PEMS08 are traffic flow datasets [Song *et al.*, 2020], while PEMS07(M), PEMS07(L) are traffic speed datasets. The statistical details of these five datasets are summarized in Table 1.

Datasets	Type	Time Interval	Node	Time Steps
PEMS04	Flow	5 min	307	16992
PEMS07	Flow	5 min	883	28224
PEMS08	Flow	5 min	170	17856
PEMS07(M)	Speed	5 min	228	12672
PEMS07(L)	Speed	5 min	1026	12672

Table 1: Summary statistics of five traffic datasets.

5.2 Baselines

We compared our model with the following 12 baselines: VAR [Lu *et al.*, 2016], STGCN [Yu *et al.*, 2018], DCRNN [Li *et al.*, 2018], ASTGCN(r) [Guo *et al.*, 2019], GWNEN [Wu *et al.*, 2019], STSGCN [Song *et al.*, 2020], AGCRN [Bai *et al.*, 2020], STFGNN [Li and Zhu, 2021], STGNCDE [Choi *et al.*, 2022], STID [Shao *et al.*, 2022a], PDFormer [Jiang *et al.*, 2023], and STAEformer [Liu *et al.*, 2023].

5.3 Performance Comparison

Table 2 shows the comparison of different models for the 1-hour ahead multi-step traffic forecasting tasks. The best results are highlighted in bold, while the second-best results are underlined. It is evident that our DST-GTN model outperforms other state-of-the-art models in all cases. These

	Models	VAR	STGCN	DCRNN	ASTGCN(r)	GWNET	STSGCN	AGCRN	STFGNN	STGNCDE	STID	PDFormer	STAEformer	DST-GTN
PEMS04	RMSE	36.39	34.77	31.43	35.22	31.72	33.65	31.25	31.87	31.09	<u>29.93</u>	30.05	30.20	29.91
	MAE	23.51	21.76	19.71	22.92	19.36	21.19	19.38	19.83	19.21	18.41	18.39	<u>18.24</u>	18.12
	MAPE (%)	17.85	13.87	13.54	16.56	13.30	13.90	13.40	13.02	12.77	12.59	12.15	<u>12.04</u>	11.91
PEMS07	RMSE	55.73	35.44	34.43	37.87	34.12	39.03	34.40	35.81	34.04	32.74	32.87	<u>32.60</u>	32.40
	MAE	37.06	22.90	21.20	24.01	21.22	24.26	20.57	22.07	20.62	19.63	19.83	<u>19.14</u>	19.00
	MAPE (%)	19.91	11.98	9.06	10.73	9.08	10.21	8.74	9.21	8.86	8.31	8.52	<u>8.01</u>	7.95
PEMS08	RMSE	31.02	27.12	24.28	28.06	24.86	26.80	24.41	26.21	24.81	23.37	23.52	<u>23.37</u>	22.91
	MAE	22.07	17.84	15.26	18.25	15.06	17.13	15.32	16.64	15.46	14.21	13.69	<u>13.54</u>	13.40
	MAPE (%)	14.04	11.21	9.96	11.64	9.51	10.96	10.03	10.55	9.92	9.29	9.07	<u>8.89</u>	8.87
PEMS07(M)	RMSE	7.61	6.79	7.18	6.18	6.24	5.93	5.54	5.79	5.39	<u>5.36</u>	5.75	5.54	5.27
	MAE	4.25	3.86	3.83	3.14	3.19	3.01	2.79	2.90	2.68	<u>2.61</u>	2.86	2.68	2.59
	MAPE (%)	10.28	10.06	9.81	8.12	8.02	7.55	7.02	7.23	6.76	<u>6.63</u>	7.18	6.70	6.59
PEMS07(L)	RMSE	8.09	6.83	8.33	6.81	7.09	6.88	5.92	5.91	<u>5.76</u>	5.78	5.90	5.93	5.69
	MAE	4.45	3.89	4.33	3.51	3.75	3.61	2.99	2.99	2.87	<u>2.81</u>	2.93	2.84	2.80
	MAPE (%)	11.62	10.09	11.41	9.24	9.41	9.13	7.59	7.69	7.31	<u>7.15</u>	7.37	7.19	7.09

Table 2: Performance comparison of DST-GTN and other baseline models. The best results are in bold and underline denotes the second-best results.

experimental results show that DST-GTN greatly improves the accuracy of traffic forecasting. The detailed experimental settings and the analysis of the advantages of DST-GTN are shown in Appendix B.2 and B.3.

5.4 Ablation Study

To assess the actual performance of each component in DST-GTN, we conducted comparisons between DST-GTN with 5 variants: w/o TT, w/o TT-ST, DST-GTN-Reverse, w/ Static Graph, w/o NFL. The definition of these variants and the ablation study results are shown in Appendix B.4.

The results lead us to the following conclusions: (1) The removal of Temporal Transformer modules and DSTM results in significant performance degradation. This highlights the importance of both temporal dependency and ST dynamics in traffic forecasting. (2) DST-GTN-Reverse performs worse than DST-GTN, suggesting that extracting ST dynamics should be based on the extraction of temporal dependencies. This structure where temporal dependencies are followed by ST dynamics aligns with the intrinsic characteristics of traffic forecasting. (3) Replacing global ST graphs with static graphs leads to a performance decrease, indicating that static graphs are inadequate for modeling the spatial relationships at different sequence positions. (4) W/o NFL performs worse than DST-GTN. This validates the effectiveness of the node frequency learning component, which can accurately identify the demands of different ST nodes for global and local information, thereby aiding in mining ST dynamics.

5.5 Model Efficiency and Robustness

Datasets	PEMS04		PEMS08	
	Inference	Training	Inference	Training
STGNCDE	15.55	150.44	11.06	107.26
PDFormer	11.07	116.90	5.02	61.11
STAEformer	6.77	66.10	3.64	37.62
DST-GTN	4.31	40.19	2.52	27.45

Table 3: Training time (s/epoch) and inference time (s) on PEMS04 and PEMS08.

We compared the computational cost of DST-GTN with the self-attention-based models PDFormer and STAEformer, and the GCN-based model STGNCDE, on the PEMS04 and PEMS08 datasets. Table 3 displays the average inference time and the average training time per epoch. In comparison with these three baseline models, DST-GTN achieves a reduction in both inference and training times by at least 36.34% and 39.20%, respectively, on the PEMS04 dataset.

Figure 3 illustrates the robustness between DST-GTN and the other three top-performing baselines on the PEMS04 and PEMS08 datasets, based on 10 experiments with different random seeds. As observed, DST-GTN typically has the shortest box in most cases, which means that DST-GTN has the best robustness.

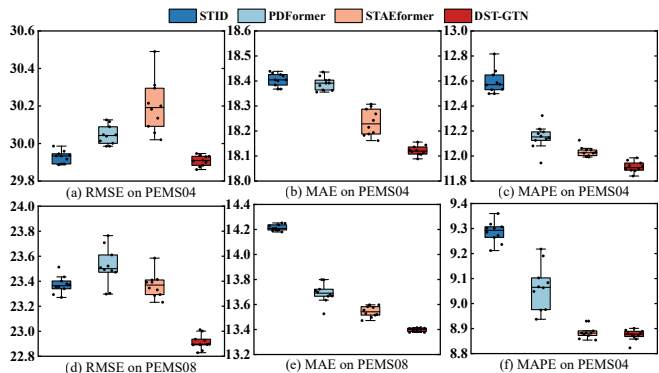


Figure 3: Robustness of different models on PEMS04 and PEMS08 datasets

6 Conclusion

In this work, we proposed a Dynamic Spatio-Temporal Graph Transformer Network (DST-GTN) for traffic forecasting. Specifically, based on the idea that ST dynamics are superimposed on temporal dependencies, DST-GTN first employed a Temporal Transformer module to extract temporal dependencies. Then, DST-GTN used Dyn-ST embedding to simulate ST dynamics and employed DSTM to dig out the in-depth ST dependency in traffic data. Extensive experiments

on five real-world traffic datasets demonstrate that our model can outperform the state-of-the-art baselines.

References

- [Atwood and Towsley, 2016] James Atwood and Don Towsley. Diffusion-convolutional neural networks. In D. Lee, M. Sugiyama, U. Luxburg, I. Guyon, and R. Garnett, editors, *Advances in Neural Information Processing Systems*, volume 29. Curran Associates, Inc., 2016.
- [Bai et al., 2020] Lei Bai, Lina Yao, Can Li, Xianzhi Wang, and Can Wang. Adaptive graph convolutional recurrent network for traffic forecasting. *Advances in neural information processing systems*, 33:17804–17815, 2020.
- [Bruna et al., 2014] Joan Bruna, Wojciech Zaremba, Arthur Szlam, and Yann LeCun. Spectral networks and locally connected networks on graphs. In Yoshua Bengio and Yann LeCun, editors, *2nd International Conference on Learning Representations, ICLR 2014, Banff, AB, Canada, April 14-16, 2014, Conference Track Proceedings*, 2014.
- [Bui et al., 2022] Khac-Hoai Nam Bui, Jiho Cho, and Hong-suk Yi. Spatial-temporal graph neural network for traffic forecasting: An overview and open research issues. *Applied Intelligence*, 52(3):2763–2774, 2022.
- [Cascetta, 2013] Ennio Cascetta. *Transportation systems engineering: theory and methods*, volume 49. Springer Science & Business Media, 2013.
- [Chen et al., 2001] Chao Chen, Karl Petty, Alexander Skabardonis, Pravin Varaiya, and Zhanfeng Jia. Freeway performance measurement system: Mining loop detector data. *Transportation Research Record*, 1748(1):96–102, 2001.
- [Choi et al., 2022] Jeongwhan Choi, Hwangyong Choi, Jeehyun Hwang, and Noseong Park. Graph neural controlled differential equations for traffic forecasting. In *Proceedings of the AAAI Conference on Artificial Intelligence*, volume 36, pages 6367–6374, 2022.
- [Defferrard et al., 2016] Michaël Defferrard, Xavier Bresson, and Pierre Vandergheynst. Convolutional neural networks on graphs with fast localized spectral filtering. In *Proceedings of the 30th International Conference on Neural Information Processing Systems, NIPS’16*, page 3844–3852, Red Hook, NY, USA, 2016. Curran Associates Inc.
- [Devlin et al., 2019] Jacob Devlin, Ming-Wei Chang, Kenton Lee, and Kristina Toutanova. BERT: Pre-training of deep bidirectional transformers for language understanding. In Jill Burstein, Christy Doran, and Thamar Solorio, editors, *Proceedings of the 2019 Conference of the North American Chapter of the Association for Computational Linguistics: Human Language Technologies, Volume 1 (Long and Short Papers)*, pages 4171–4186, Minneapolis, Minnesota, June 2019. Association for Computational Linguistics.
- [Drucker et al., 1996] Harris Drucker, Chris J. C. Burges, Linda Kaufman, Alex Smola, and Vladimir Vapnik. Support vector regression machines. In *Proceedings of the 9th International Conference on Neural Information Processing Systems, NIPS’96*, page 155–161, Cambridge, MA, USA, 1996. MIT Press.
- [Guo et al., 2019] Shengnan Guo, Youfang Lin, Ning Feng, Chao Song, and Huaiyu Wan. Attention based spatial-temporal graph convolutional networks for traffic flow forecasting. *Proceedings of the AAAI Conference on Artificial Intelligence*, 33(01):922–929, Jul. 2019.
- [Hamilton et al., 2017] Will Hamilton, Zitao Ying, and Jure Leskovec. Inductive representation learning on large graphs. *Advances in neural information processing systems*, 30, 2017.
- [Jiang et al., 2023] Jiawei Jiang, Chengkai Han, Wayne Xin Zhao, and Jingyuan Wang. Pdfformer: Propagation delay-aware dynamic long-range transformer for traffic flow prediction. *Proceedings of the AAAI Conference on Artificial Intelligence*, 37(4):4365–4373, Jun. 2023.
- [Jin et al., 2023a] Di Jin, Jiayi Shi, Rui Wang, Yawen Li, Yuxiao Huang, and Yu-Bin Yang. Trafformer: unify time and space in traffic prediction. In *Proceedings of the AAAI Conference on Artificial Intelligence*, volume 37, pages 8114–8122, 2023.
- [Jin et al., 2023b] Guangyin Jin, Yuxuan Liang, Yuchen Fang, Zezhi Shao, Jincan Huang, Junbo Zhang, and Yu Zheng. Spatio-temporal graph neural networks for predictive learning in urban computing: A survey. *IEEE Transactions on Knowledge and Data Engineering*, 2023.
- [Ju et al., 2022] Mingxuan Ju, Shifu Hou, Yujie Fan, Jianan Zhao, Yanfang Ye, and Liang Zhao. Adaptive kernel graph neural network. *Proceedings of the AAAI Conference on Artificial Intelligence*, 36(6):7051–7058, Jun. 2022.
- [Kipf and Welling, 2017] Thomas N. Kipf and Max Welling. Semi-supervised classification with graph convolutional networks. In *5th International Conference on Learning Representations, ICLR 2017, Toulon, France, April 24-26, 2017, Conference Track Proceedings*. OpenReview.net, 2017.
- [LeCun et al., 2015] Yann LeCun, Yoshua Bengio, and Geoffrey Hinton. Deep learning. *nature*, 521(7553):436–444, 2015.
- [Li and Zhu, 2021] Mengzhang Li and Zhanxing Zhu. Spatial-temporal fusion graph neural networks for traffic flow forecasting. In *Proceedings of the AAAI conference on artificial intelligence*, volume 35, pages 4189–4196, 2021.
- [Li et al., 2018] Yaguang Li, Rose Yu, Cyrus Shahabi, and Yan Liu. Diffusion convolutional recurrent neural network: Data-driven traffic forecasting. In *International Conference on Learning Representations*, 2018.
- [Liu et al., 2021] Ze Liu, Yutong Lin, Yue Cao, Han Hu, Yixuan Wei, Zheng Zhang, Stephen Lin, and Baining Guo. Swin transformer: Hierarchical vision transformer using shifted windows. In *Proceedings of the IEEE/CVF international conference on computer vision*, pages 10012–10022, 2021.

- [Liu *et al.*, 2023] Hangchen Liu, Zheng Dong, Renhe Jiang, Jiewen Deng, Jinliang Deng, Qunjun Chen, and Xuan Song. Spatio-temporal adaptive embedding makes vanilla transformer sota for traffic forecasting. In *Proceedings of the 32nd ACM International Conference on Information and Knowledge Management*, pages 4125–4129, 2023.
- [Lu *et al.*, 2016] Zheng Lu, Chen Zhou, Jing Wu, Hao Jiang, and Songyue Cui. Integrating granger causality and vector auto-regression for traffic prediction of large-scale w lans. *KSII Transactions on Internet & Information Systems*, 10(1), 2016.
- [Lv *et al.*, 2014] Yisheng Lv, Yanjie Duan, Wenwen Kang, Zhengxi Li, and Fei-Yue Wang. Traffic flow prediction with big data: A deep learning approach. *IEEE Transactions on Intelligent Transportation Systems*, 16(2):865–873, 2014.
- [Park *et al.*, 2020] Cheonbok Park, Chunggi Lee, Hyojin Bahng, Yunwon Tae, Seungmin Jin, Kihwan Kim, Sungahn Ko, and Jaegul Choo. St-grat: A novel spatio-temporal graph attention networks for accurately forecasting dynamically changing road speed. In *Proceedings of the 29th ACM international conference on information & knowledge management*, pages 1215–1224, 2020.
- [Ruan *et al.*, 2022] Bo-Kai Ruan, Hong-Han Shuai, and Wen-Huang Cheng. Vision transformers: State of the art and research challenges. *CoRR*, abs/2207.03041, 2022.
- [Shao *et al.*, 2022a] Zezhi Shao, Zhao Zhang, Fei Wang, Wei Wei, and Yongjun Xu. Spatial-temporal identity: A simple yet effective baseline for multivariate time series forecasting. In *Proceedings of the 31st ACM International Conference on Information & Knowledge Management*, pages 4454–4458, 2022.
- [Shao *et al.*, 2022b] Zezhi Shao, Zhao Zhang, Wei Wei, Fei Wang, Yongjun Xu, Xin Cao, and Christian S. Jensen. Decoupled dynamic spatial-temporal graph neural network for traffic forecasting. *Proc. VLDB Endow.*, 15(11):2733–2746, jul 2022.
- [Song *et al.*, 2020] Chao Song, Youfang Lin, Shengnan Guo, and Huaiyu Wan. Spatial-temporal synchronous graph convolutional networks: A new framework for spatial-temporal network data forecasting. In *Proceedings of the AAAI conference on artificial intelligence*, volume 34, pages 914–921, 2020.
- [Van Lint and Van Hinsbergen, 2012] JWC Van Lint and CPIJ Van Hinsbergen. Short-term traffic and travel time prediction models. *Artificial Intelligence Applications to Critical Transportation Issues*, 22(1):22–41, 2012.
- [Vaswani *et al.*, 2017] Ashish Vaswani, Noam Shazeer, Niki Parmar, Jakob Uszkoreit, Llion Jones, Aidan N Gomez, Łukasz Kaiser, and Illia Polosukhin. Attention is all you need. *Advances in neural information processing systems*, 30, 2017.
- [Veličković *et al.*, 2018] Petar Veličković, Guillem Cucurull, Arantxa Casanova, Adriana Romero, Pietro Liò, and Yoshua Bengio. Graph attention networks. In *International Conference on Learning Representations*, 2018.
- [Weng *et al.*, 2023] Wenchao Weng, Jin Fan, Huifeng Wu, Yujie Hu, Hao Tian, Fu Zhu, and Jia Wu. A decomposition dynamic graph convolutional recurrent network for traffic forecasting. *Pattern Recognition*, 142:109670, 2023.
- [Williams and Hoel, 2003] Billy M. Williams and Lester A. Hoel. Modeling and forecasting vehicular traffic flow as a seasonal arima process: Theoretical basis and empirical results. *Journal of Transportation Engineering*, 129(6):664–672, 2003.
- [Wu *et al.*, 2019] Zonghan Wu, Shirui Pan, Guodong Long, Jing Jiang, and Chengqi Zhang. Graph wavenet for deep spatial-temporal graph modeling. In *Proceedings of the Twenty-Eighth International Joint Conference on Artificial Intelligence, IJCAI-19*, pages 1907–1913. International Joint Conferences on Artificial Intelligence Organization, 7 2019.
- [Yao *et al.*, 2018] Huaxiu Yao, Fei Wu, Jintao Ke, Xianfeng Tang, Yitian Jia, Siyu Lu, Pinghua Gong, Jieping Ye, and Zhenhui Li. Deep multi-view spatial-temporal network for taxi demand prediction. In *Proceedings of the AAAI conference on artificial intelligence*, volume 32, 2018.
- [Yu *et al.*, 2018] Bing Yu, Haoteng Yin, and Zhanxing Zhu. Spatio-temporal graph convolutional networks: A deep learning framework for traffic forecasting. In *Proceedings of the Twenty-Seventh International Joint Conference on Artificial Intelligence, IJCAI-18*, pages 3634–3640. International Joint Conferences on Artificial Intelligence Organization, 7 2018.
- [Zheng *et al.*, 2020] Chuanpan Zheng, Xiaoliang Fan, Cheng Wang, and Jianzhong Qi. Gman: A graph multi-attention network for traffic prediction. *Proceedings of the AAAI Conference on Artificial Intelligence*, 34(01):1234–1241, Apr. 2020.

A Details of DST-GTN

A.1 Temporal Identity Embedding.

To obtain two temporal identities E^{week} and E^{day} , we define a learnable parameter $I^{day} \in \mathbb{R}^{T^d \times d_1}$ and another learnable parameter $I^{week} \in \mathbb{R}^{T^w \times d_1}$ for identifying each sampling time within a day and each day within a week, respectively. Here, T^d depends on the number of traffic data samples collected within a day, which typically is equal to 288, while T^w is equal to 7. Subsequently, the original temporal information of each input traffic data will be mapping to corresponding daily periodicity representation among I^{day} and weekly periodicity representation among I^{week} . The mapping result, E^{week} and E^{day} , can be used to jointly identify temporal characteristics of each time slice of input traffic data.

A.2 Algorithm of DST-GTN

We summarize the overall computation process of DST-GTN as the following Algorithm 1.

Algorithm 1 The overall algorithm of DST-GTN

Input: The traffic data sequence over the past T time steps \mathcal{X} and their corresponding time stamp.

Output: The forecasting of future traffic data sequence \mathcal{Y} .

- 1: Initialize E^{day} and E^{week} based on time stamp.
 - 2: Initialize E^{st} randomly.
 - 3: $\mathcal{H} \leftarrow MLP(\mathcal{X})$
 - 4: $\mathcal{Z}^{(0)} \leftarrow \mathcal{H} \| E^{day} \| E^{week} \| E^{st}$
 - 5: **for** l in range(L) **do**
 - 6: $\hat{\mathcal{Z}}^{(l)} = LayerNorm(MTSA(\mathcal{Z}^{(l-1)}) + \mathcal{Z}^{(l-1)})$
 - 7: $\mathcal{Z}^{(l)} = LayerNorm(FFN(\hat{\mathcal{Z}}^{(l)}) + \hat{\mathcal{Z}}^{(l)})$
 - 8: **end for**
 - 9: $\mathcal{Z}^{(0)} \leftarrow \mathcal{Z}^{(L)}$
 - 10: **for** l in range(L) **do**
 - 11: Calculate $A_{local}^{st(l)}$ and $A_{global}^{st(l)}$ according to Eq. 13 - Eq. 20.
 - 12: $\hat{\mathcal{Z}}^{(l)} \leftarrow (A_{local}^{st(l)} + A_{global}^{st(l)}) \times \mathcal{Z}^{(l-1)} W$
 - 13: $\mathcal{Z}^{(l)} \leftarrow LayerNorm(\hat{\mathcal{Z}}^{(l)} + \mathcal{Z}^{(l-1)})$
 - 14: **end for**
 - 15: $\mathcal{Y} \leftarrow MLP(\mathcal{Z}^{(L)})$
-

B Details of Experiment

B.1 Baseline

- VAR is an classic time series method, which capture the pairwise correlations among time series.
- STGCN utilizes temporal convolution network (TCN) and GCN to capture temporal dependencies and spatial dependencies in traffic data, respectively.
- DCRNN captures the spatial dependency using bidirectional random walks on the graph, and the temporal dependency using the encoder-decoder architecture with scheduled sampling.
- ASTGCN(r) combines an attention mechanism with graph convolution to model traffic data.

- GWNET uses Gated TCN and GCN to model the temporal dependencies and spatial dependencies in traffic data, respectively, and introduces a self-adaptive adjacency matrix to learn spatial adjacency relationships.
- STSGCN captures the complex localized spatial-temporal correlations through spatial-temporal synchronous modeling mechanism.
- AGCRN integrates GCN into the computational process of RNN to model time-varying spatial relationship.
- STFGNN synchronously captures the ST correlation through the fusion of multiple spatial and temporal graphs.
- STGNCDE extends the concept of neural controlled differential equations to temporal processing and spatial processing in traffic data.
- STID designs multiple embedding and use simple multi-layer perceptrons to forecast traffic data.
- PDFormer utilizes multiple self-attention mechanism from spatial and temporal perspectives to achieve traffic forecasting.
- STAEformer utilizes Vanilla Transformer from both temporal and spatial perspectives and introduces multiple embeddings.

B.2 Settings

Dataset Processing. Consistent with previous research [Song *et al.*, 2020; Weng *et al.*, 2023; Jiang *et al.*, 2023], we divided all five datasets in chronological order, allocating 60% for training, 20% for validation, and 20% for testing, following a 6:2:2 ratio. Previous 12 time steps traffic data were used to forecast the traffic data for the next 12 time steps, i.e., an equal-length multi-step forecasting. All datasets were normalized by Z-score normalization to standardize the inputs.

Hyper-parameters. The embedding dimension of E^{day}, E^{week} , and \mathcal{H} was set to 24. The embedding dimension of E^{st} was set to 80. All number of multi-head attention heads were set to 4. The number of both Temporal Transformer module and DSTM were set to 3. We trained our model by using Adam optimizer and the training epoch was set to 200. The learning rate was set to 0.001 and the batch size was equal to 16. Additionally, early stopping strategy was used to avoid overfitting. We used the mean absolute error (MAE) as loss function to train our model.

Evaluation Metric. We adopted three metrics to evaluate the performance of model: the first one is Mean Absolute Error (MAE), the second one is Root Mean Square Error (RMSE), and the third one is Mean Absolute Percentage Error (MAPE). Missing values in the data were not be considered during the evaluation process.

Platform. All experiments were conducted on a machine equipped with an NVIDIA GeForce 3090 GPU. DST-GTN was implemented using Pytorch 1.12.1 and Python 3.9.12. All experiments were repeated 10 times with different random seeds and the average results were reported.

B.3 Analysis of Comparison Experiment

VAR considers only the temporal dependency of traffic time-series data but ignores the crucial spatial information. Models like STGCN, ASTGCN(r), GWNEN, STGCNDE address both temporal and spatial dependencies using two separate modules, respectively. However, they overlook the dynamic ST interactions in traffic time-series data.

To modeling ST dynamics, DCRNN and AGCRN integrate GNN with RNN to simulate time-varying spatial relationships. In contrast, STSGCN and STFGNN utilize pre-defined ST graphs to represent ST relationships over multiple steps. Among these, DCRNN, STSGCN, and STFGNN employ pre-defined graph structures, potentially introducing incorrect prior knowledge into the models. AGCRN employs learnable node embedding to adaptively learn the graph structure and demonstrates better result. DST-GTN achieves better performance by learning ST dynamics through Dyn-ST embedding without relying on any prior knowledge.

STID exhibits exceptional performance using only a MLP combined with temporal and spatial embedding. This proves the effectiveness of well-applied embedding. PDFormer and STAEformer are entirely relied on self-attention and show promising result on traffic forecasting, which indicate the positive impact of self-attention mechanism. However, both STID, PDFormer, and STAEformer overlook the precise modeling of ST dynamics. For instance, STAEformer applies learnable ST embedding to traffic data but does not fully exploit them. In contrast, DST-GTN employs the self-attention mechanism to capture the information from Dyn-ST embedding. The generated ST graph integrates both observed global and local information demands of each ST nodes to represent ST dynamics.

Another key factor contributing to the superior performance of DST-GTN is its well-considered architectural design. The previously mentioned baseline models often concentrate on extracting spatial dependencies after temporal dependencies or on extracting both temporal and spatial dependencies. In contrast, DST-GTN goes a step further by extracting ST dynamics on top of temporal dependencies, which is intuitively more consistent with the characteristics of traffic time-series data.

B.4 Details of Ablation Study

Datasets	PEMS04			PEMS08		
	RMSE	MAE	MAPE(%)	RMSE	MAE	MAPE(%)
w/o TT	31.35	19.73	14.18	24.56	15.43	10.86
w/o TT-ST	39.89	25.17	18.00	31.49	19.96	18.52
DST-GTN Reverse	30.01	18.34	12.02	23.19	13.74	9.09
w/ Static Graph	30.05	18.34	12.10	23.06	13.64	9.10
w/o NFL	30.08	18.29	12.17	23.20	13.54	9.13
DST-GTN	29.91	18.12	11.91	22.91	13.40	8.87

Table 4: Ablation study on PEMS04 and PEMS08 datasets.

The definition of different variants in ablation study are described as follows:

- (1)**w/o TT**: It removes Temporal Transformer module.
- (2)**w/o TT-ST**: It removes Temporal Transformer module and Dynamic Spatio-Temporal Module.

(3)**DST-GTN-Reverse**: It reverses the order of Temporal Transformer module and Dynamic Spatio-Temporal Module.

(4)**w/ Static Graph**: It replaces global ST graph generated by DSTGG with static graph generated by distance between traffic nodes.

(5)**w/o NFL**: It removes the Node Frequency Learning component.

Table A presents a comparison of these variants on the PEMS04 and PEMS08 datasets.

C Traffic Forecasting Visualization

In this section, we visualize the ground truth and some forecasting outcomes by our method and STAEformer in Figure 4.

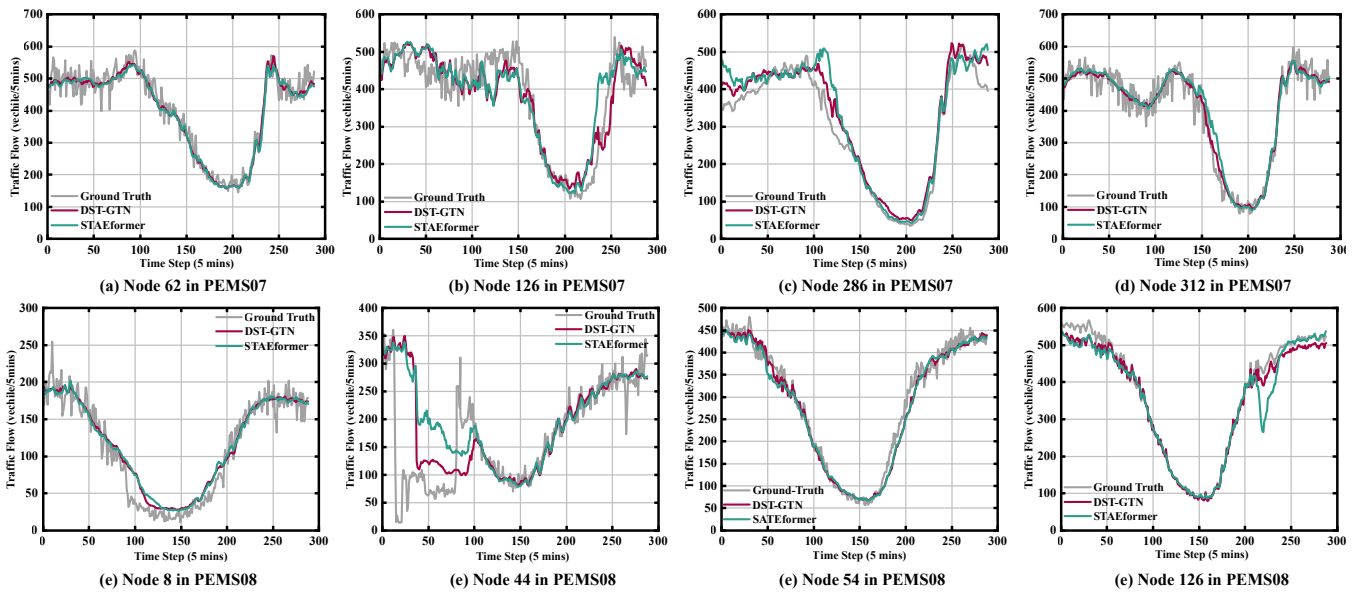


Figure 4: Traffic forecasting visualization.